THE DEFORMATION BEHAVIOR OF P/M RENE'95

UNDER ISOTHERMAL FORGING CONDITIONS

J. M. Morra, R.R. Biederman, F.R. Tuler

Mechanical Engineering Department
Worcester Polytechnic Institute
Worcester, MA 01609

Abstract

The high temperature deformation behavior of as-HIP P/M Rene'95 as a function of powder particle size has been examined. Compression testing of +230, -270+400, and -500 mesh materials at temperatures of 1038°C, 1079°C, and 1121°C and constant true strain rates of 10^{-1}, 1, and 5 s^{-1} has shown there to be virtually no difference in their flow behavior. All three materials exhibited a rapid work-hardening to a peak flow stress, followed by a gradual flow softening which approached a steady-state of flow stress at a true strain of 0.50. Peak flow stress, rate of flow softening, steady-state flow stress, and strain at the onset of steady-state flow were all seen to increase with increased strain rate and/or decreased temperature. With lowered temperature and increased strain rate the as-HIP materials exhibited non-uniform deformation which was attributed to strain gradients created within the material at prior powder particles. Deformation maps created from compression test data predict processing instability over most of the temperature/strain rate range of this study.

Introduction

The deformation behavior of various P/M nickel-base superalloys has been studied by several researchers (1,2,3,4). The goal of this work has been to define the processing parameters which result in the optimum workability of these P/M materials. A new approach to this issue was developed (5), whereby dynamic material behavior is modeled in terms of the efficiency of energy dissipation in a workpiece during processing, as a function of temperature and strain rate. This model, known also as a deformation map, can be utilized as an aide in choosing optimum processing parameters, provided that metallurgical processes corresponding to the projected efficiencies across the map are known (6).

This paper describes a study made of the high temperature deformation behavior of as-HIP P/M Rene'95, as a function of initial powder particle size, and attempts made to generate corresponding deformation maps. Particular attention will be given to discussing some of the problems encountered with the creation and interpretation of such maps.

Superalloys 1988
Edited by S. Reichman, D.N. Duhl,
G. Maurer, S. Antolovich and C. Lund
The Metallurgical Society, 1988

Experimental Procedure

Argon atomized P/M Rene'95 powder (Table I) was screened into three size lots of +230, -270 + 400, and -500 mesh. Each size lot was compacted by hot isostatic pressing (HIP) at 1121°C, 103 MPa, for three hours. Gamma prime solvus was determined by DTA to be ~1159°C.

Compression specimens measuring 1.0 cm in diameter and 1.5 cm in height were machined from the as-HIP material. Shallow spiral grooves were made in the ends of the specimens for lubricant retention at hot-working temperatures. The specimens were coated with a boron nitride lubricant. Because of the limited amount of material, the test matrix consisted of only three temperatures and three strain rates. Compression testing was conducted at temperatures of 1038°C, 1079°C, and 1121°C and strain rates of 10^{-1},1, and 5 s^{-1}. The compression tests were performed on a 222 kN servohydraulic Instron testing system equipped with a three-zone ATS split-type resistance furnace. Each specimen was held at temperature for at least 15 minutes prior to compression, to allow for uniform heating throughout the specimen. Specimens were compressed between silicon nitride flat dies mounted on Udimet 720 compression columns, to a total true strain of 0.50, and were immediately water quenched. Constant true strain rate was maintained by an analog exponential function generator. Load-time and stroke-time data were recorded on a digital oscilloscope and were plotted as load-stroke curves on an X-Y recorder. The data were replotted in terms of stress and strain using standard equations, assuming uniform deformation and a constant specimen volume.

Microstructures of the three starting materials and each of the compression specimens were examined for gamma prime distribution and prior particles using SEM . TEM was used to determine gamma prime size distribution and morphology.

Table I. Chemical Analysis of P/M Rene'95* (in Wt. %)

Ni	Cr	Co	Mo	W	Nb	Al	Ti	C	B	Zr	O (ppm)
Bal	13.15	8.44	3.36	3.39	3.52	3.37	2.32	0.06	-	0.05	83

*Rene'95 is a trademark of the General Electric Co.

Experimental Results

Flow Curves

The flow curves for the three materials tested are shown in Figures 1 and 2. As seen in these figures, the flow behavior appears to be independent of particle size. All three materials exhibit rapid work-hardening to a peak flow stress, followed by a gradual flow softening which approaches a steady-state of flow stress at a true strain of 0.50. Peak flow stress, rate of flow softening, steady-state flow stress, and strain at the onset of steady-state flow all increase with increased strain rate and/or decreased temperature.

Peak flow stress data were obtained from the flow curves and are plotted versus strain rate and as a function of temperature in Figure 2. These data were utilized to calculate strain rate sensitivity, m, defined as:

$$m = \frac{d\ln\sigma}{d\ln\dot{\epsilon}} \qquad (1)$$

In order to calculate m, the logarithm of the peak flow stress versus the logarithm of strain rate was plotted based on a polynomial regression fit. The equation of the curve corresponding to

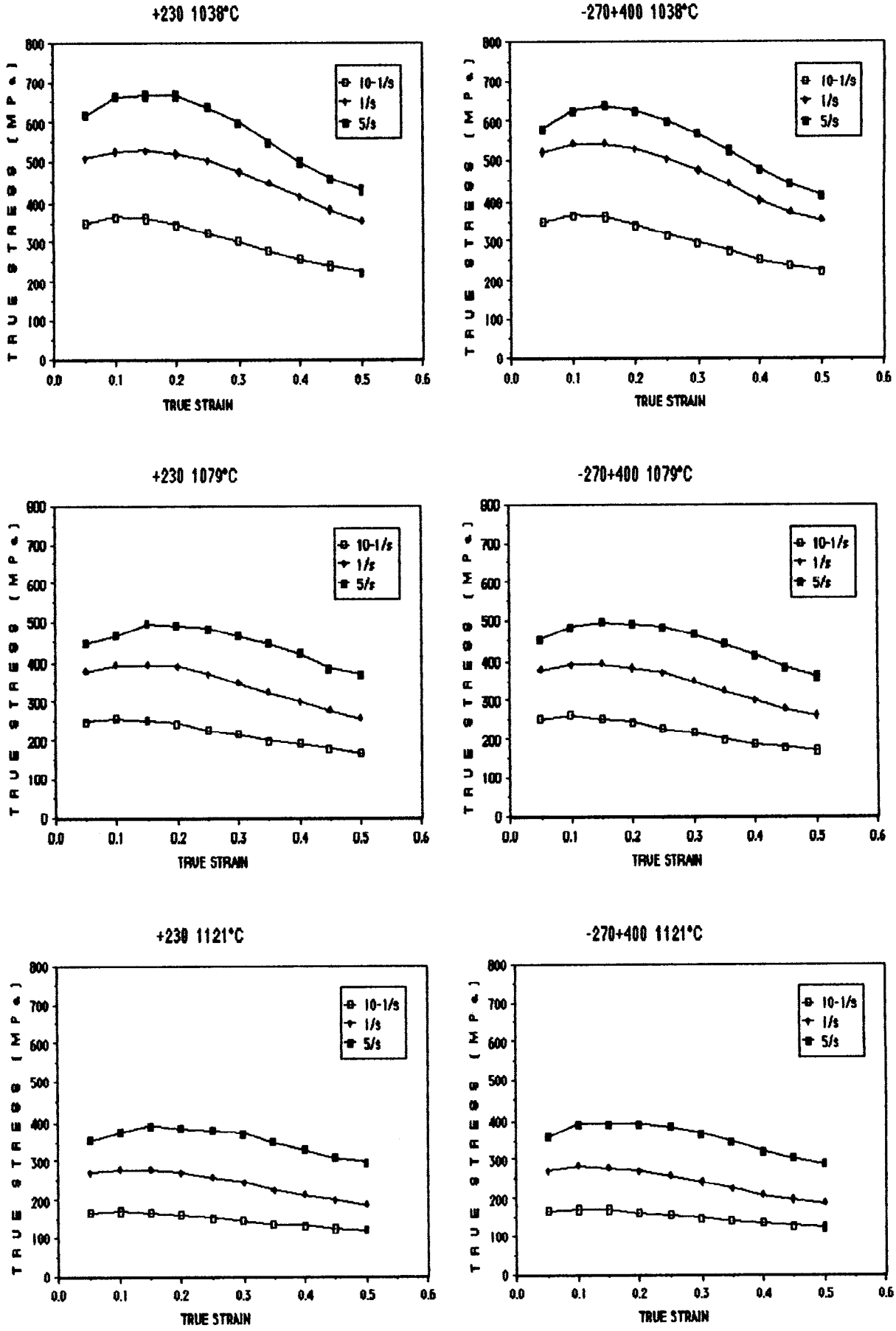

Figure 1. $\sigma - \varepsilon$ Curves as a function of temperature.

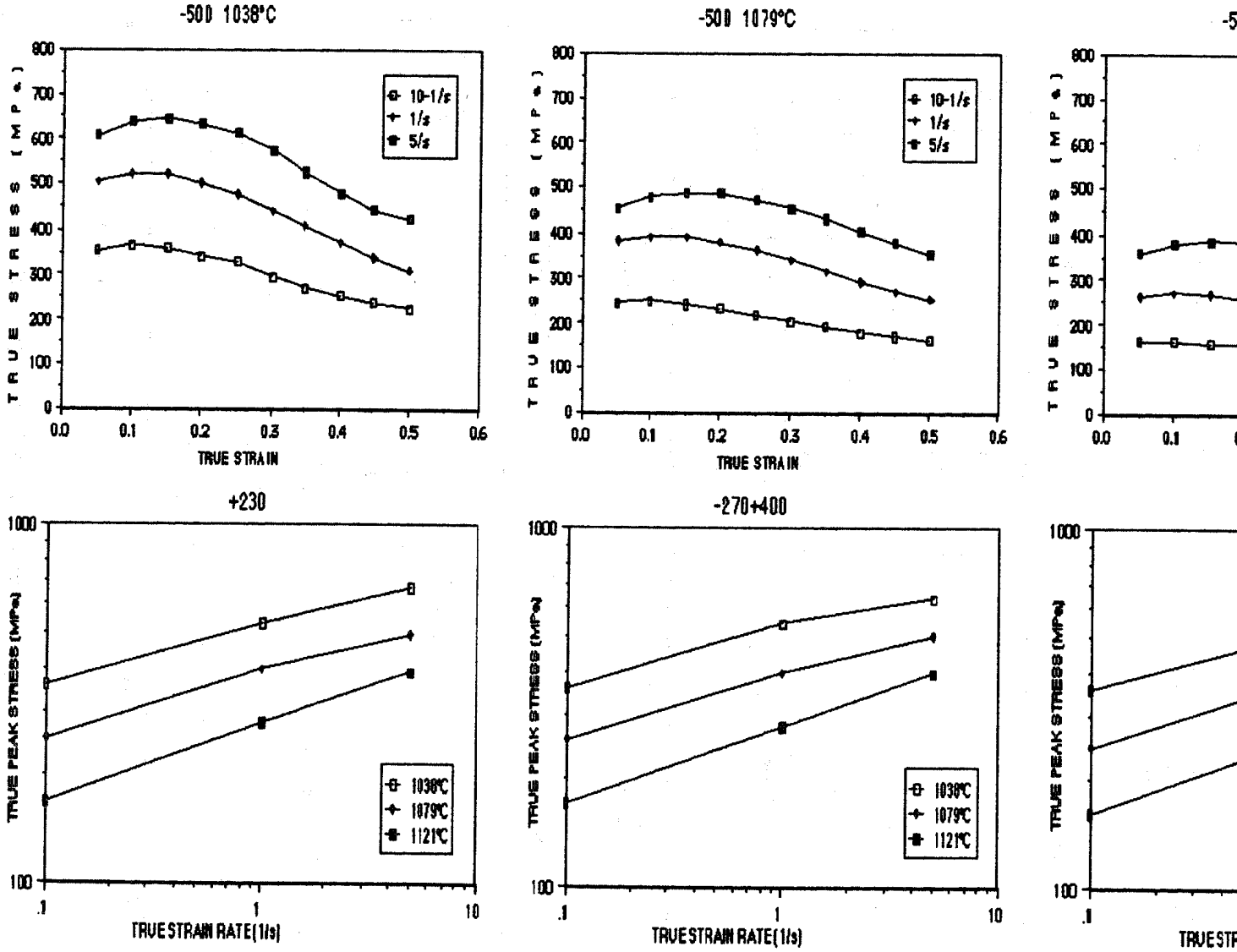

Figure 2. Top row: σ - ε curves, -500 mesh. Bottom row: log σ_{peak} vs. log

the polynomial fit was differentiated to give the equation for the slope of the curve at any given point. Thus, m could be calculated at each strain rate. Table II lists the strain rate sensitivities calculated in this manner for a second order polynomial fit, all of which have values of $m < 0.3$. Superplastic behavior is typified by strain rate sensitivities in the range of 0.3 - 0.8, corresponding to stage II on the sigmoidal $\ln \sigma - \ln \dot{\varepsilon}$ curve, where deformation occurs by grain boundary or interphase boundary sliding. The values presented in Table II are characteristic of stage III on the $\ln \sigma - \ln \dot{\varepsilon}$ curve, where deformation occurs by intragranular flow, and conventional hot-working mechanisms such as dynamic recovery and dynamic recrystallization operate (2). As seen in Table II, there does not appear to be a transition to stage II deformation over the range of strain rates tested.

Table II Strain Rate Sensitivity at Peak Stress As a Function of Temperature and Strain Rate

Powder Size	Temperature (°C)	Strain Rate (s^{-1})		
		10^{-1}	1	5
+230	1038	0.18	0.16	0.14
	1079	0.22	0.16	0.12
	1121	0.22	0.21	0.20
-270+400	1038	0.23	0.13	0.06
	1079	0.21	0.16	0.13
	1121	0.22	0.22	0.22
-500	1038	0.18	0.14	0.12
	1079	0.23	0.16	0.12
	1121	0.21	0.22	0.23

There was a tendency for some of the test specimens to deform non-uniformly – i.e. the geometry of a right circular cylinder with parallel sides was not maintained. This tendency was seen to increase with increased strain rate or decreased temperature. Non-uniformity was in most cases accompanied by edge-cracking of the specimens.

Deformation Maps

A deformation map is a plot of the calculated efficiency of power dissipated during plastic deformation, as a function of temperature and strain rate, for a given strain. Efficiency is defined (5) as:

$$\eta = \frac{2m}{(m+1)} \qquad (2)$$

where m = strain rate sensitivity.

Deformation maps corresponding to a true strain of 0.50 were generated. Flow stress data corresponding to 0.50 strain were used to calculate m values in the same manner as cited previously. As there were only three strain rates involved, a second-order polynomial regression fit of the data was initially chosen, and was subsequently compared to a linear fit.

Values of m calculated from a linear regression curve fit of the data indicate no superplasticity ($m < 0.3$), and constant strain rate sensitivity. A second-order polynomial fit indicates that the materials were deforming superplastically (at true strain = 0.50) at the highest strain rate and highest temperature of this study ($m >= 0.3$). The possibility of superplasticity occurring at a strain rate of 5 s^{-1} appears unlikely. Curve fitting of log flow stress vs. log strain

rate data based on only three data points (three strain rates) is assumed to be the basis for this discrepancy. Efficiency values calculated from these strain rate sensitivities are shown in Table III.

Deformation maps generated from the polynomial fit data are shown in Figure 3. Maps based on a second-order polynomial fit, in general, indicate an increase in efficiency with increased strain rate. A linear fit would force the maps to have a constant efficiency over the range of strain rates at each temperature. In either case, efficiency increases with increased temperature. It is obvious that the generation of deformation maps can be sensitive to the method of data manipulation chosen.

In addition to predicting conditions of high processing efficiency, deformation maps delineate regions of "stable" processing for a workpiece. Stability of a workpiece under a given set of conditions is a concept which implies that "safe" processing may result – that no unfavorable processes which produce defects, fracture, or plastic instability will occur. Stability is represented in two parts, which are defined as follows (7):

$$\text{Mechanical Stability} \qquad \frac{d\eta}{d\log\dot{\varepsilon}} \qquad (3)$$

$$\text{Material Stability} \qquad \frac{ds}{d\log\dot{\varepsilon}} \qquad (4)$$

where

$$s = \frac{1}{T}\left[\frac{d\log\sigma}{dT^{-1}}\right] \qquad (5)$$

and T = absolute temperature.

In order for a process to be considered stable, equations 3 and 4 must be negative. Based on these criteria, the deformation maps shown in Figure 3 predict processing instability over most of the temperature - strain rate range used for this study.

Microstructural Analysis

Microstructural analysis of the starting materials and the compressed specimens was conducted to correlate predicted processing stability with microstructure. Microstructures of the three starting materials, shown in Figure 4, indicate the presence of prior powder particles after HIP. Prior powder particle areas are characterized by a globular, interdendritic distribution of gamma prime and are outlined by a course gamma prime precipitate. Areas surrounding prior particles contain a random distribution of gamma prime of varying size fractions. Examination of the microstructures at all test conditions after deformation to a true strain of 0.50 showed the three materials to be microstructurally similar. Each sample had undergone grain refinement via dynamic recrystallization, and exhibited a more homogeneous microduplex gamma + gamma prime structure. Gamma prime was seen to have coarsened with increased temperature, resulting in a larger recrystallized grain size at higher temperatures. Prior powder particles were noted to be present after deformation in all three materials, under all test conditions. The microstructure of the prior powder particles was noticeably different from that of the regions surrounding them, as illustrated in Figure 5. The interdendritic powder particle areas contained a high dislocation density which had not been present in the as-HIP material prior to compression, and showed no signs of having undergone recrystallization. The regions

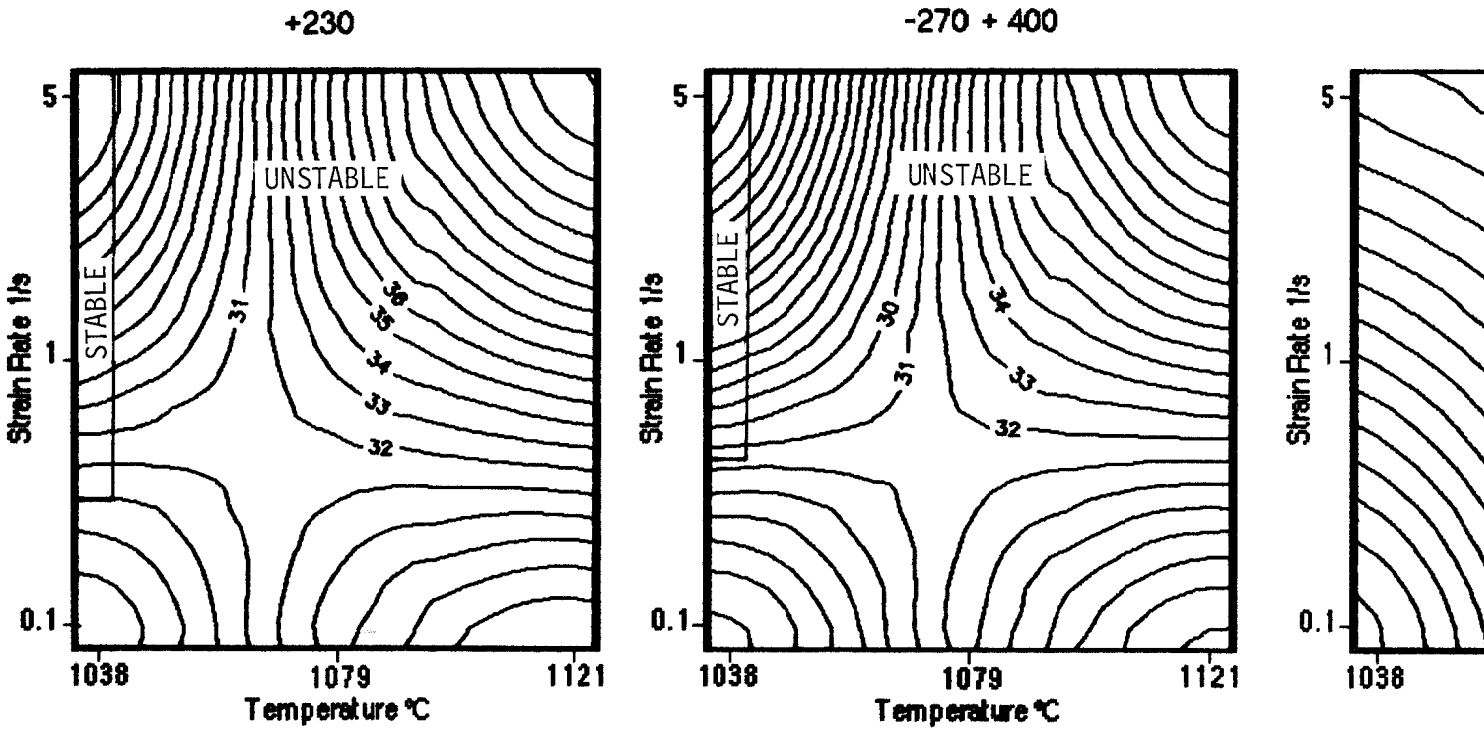

Figure 3. Deformation maps of the three materials at $\varepsilon = 0.5$.

Table III. Efficiency (%) as a Function of Temperature, Strain Rate, and Method of Data Fit

Size	Temp. (°C)	Strain Rate (s^{-1})					
		10^{-1}		1		5	
		2nd Order	Linear	2nd Order	Linear	2nd Order	Linear
+230	1038	37.4	28.6	26.7	28.6	18.3	28.6
	1079	28.7	33.3	34.2	33.3	37.9	33.3
	1121	24.6	36.6	38.9	36.6	47.6	36.6
-270+400	1038	39.3	27.3	24.5	27.3	12.4	27.3
	1079	29.8	32.6	33.2	32.6	35.5	32.6
	1121	23.1	35.3	37.6	35.3	46.5	35.3
-500	1038	20.4	27.9	29.4	27.9	35.2	27.9
	1079	29.9	33.0	33.6	33.0	36.2	33.0
	1121	27.3	36.8	38.7	36.8	45.8	36.8

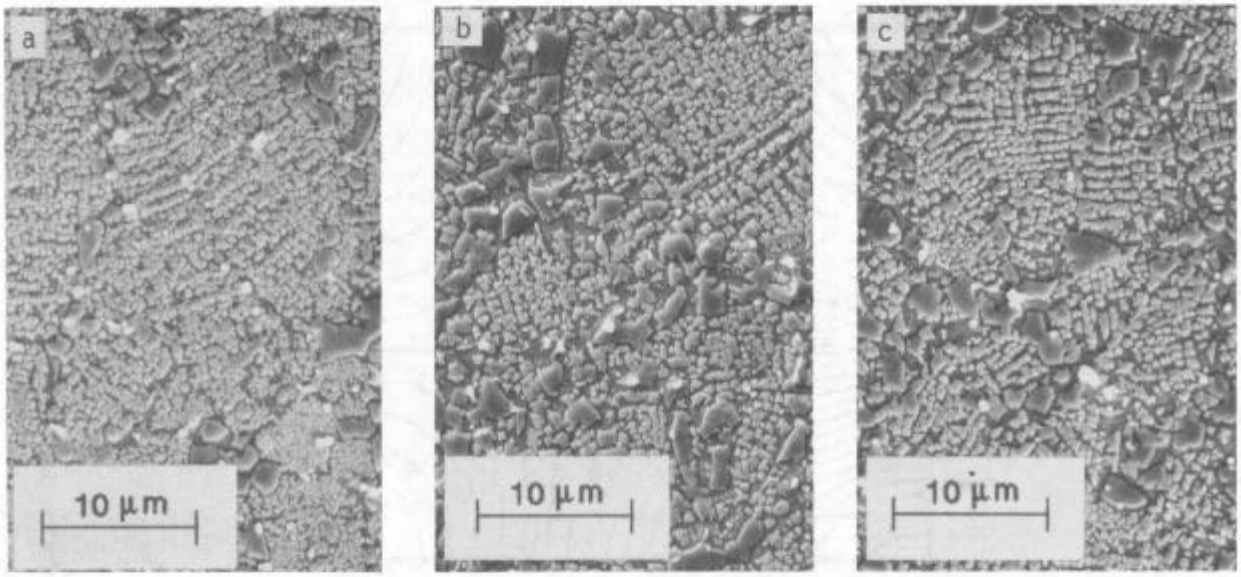

Figure 4. SEM micrographs of as-HIP materials: (a) +230 mesh, (b) -270+400 mesh, (c) -500 mesh.

surrounding prior powder particles were dynamically recrystallized and virtually dislocation-free. These observations support the theory that material flow occurred primarily in the regions surrounding prior particles, with very little flow taking place within the particles themselves. Flow that did occur within the prior particles resulted in the creation of dendritic remnants. Examination of the microstructure of a specimen which had undergone non-uniform deformation revealed edge cracks that followed the contour of prior powder particles, with voids at points of particle decohesion. No evidence of shear banding was noted in any of the specimens.

Discussion.

From the data presented in this study, it is apparent that little discernable difference exists between the flow behavior of as-HIP P/M Rene'95 as a function of starting powder particle size.

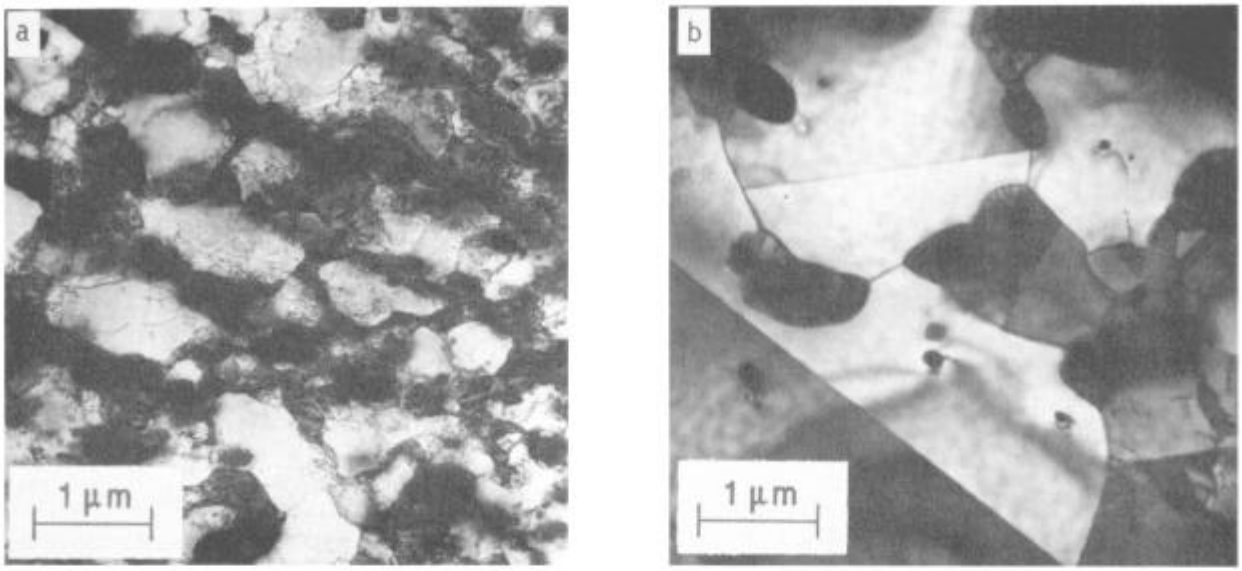

Figure 5. TEM microstructural comparison of (a) prior powder particle and (b) surrounding recrystallized area

Observed deformation behavior of the as-HIP materials is consistent with the findings of others (1,2,3,4). Correlation of strain rate sensitivities and microstructural observations leads to the conclusion that deformation over the given range of temperatures and strain rates is of the stage III type, characterized by intragranular flow, dynamic recovery and dynamic recrystallization. The tendency toward non-uniform flow behavior of all three materials with increased strain rate or decreased temperature is thought to be due to the inhomogeneous nature of the material itself. Specifically, the presence of dendritic prior powder particles introduces strain gradients in the material which cannot be accommodated at high strain rates and low temperatures, resulting in cracks and decohesion at prior particle boundaries. In general, prior particles undergo relatively little deformation, while the material surrounding them flows and dynamically recrystallizes.

Interpretation of the generated deformation maps in terms of the observations made above is unclear. Maps based on a second order polynomial fit of stress-strain data in some instances imply superplasticity, while those based on a linear fit do not. The latter case may seem to be a more realistic model, yet a polynomial fit is cited (8) as being the correct method for creating deformation maps. Maps based on more than three strain rates would provide more insight in this regard.

Both types of maps predict processing instability for the three materials over most, if not all of the temperature-strain rate range of this study. Because both parts of the stability criterion must be true in order for a map region to be deemed "unstable", the specific component that causes system instability may not be discernable. It is therefore difficult to know the nature of the instability predicted in the deformation maps. The non-uniform flow behavior observed could be assumed to be the predicted instability, yet two of the most severe cases occurred under conditions which were within stable regions of the deformation maps

Microstructural analysis showed that all of the compressed specimens had undergone substantial grain refinement, with some prior powder particle refinement, and a phase redistribution that resulted in a more homogeneous structure. Such microstructural change is generally considered favorable, yet the maps designate such processing to be unstable. It is unclear whether stability should be interpreted as being desirable for processing, especially since it does not seem to correlate with microstructure.

Based on this study, future work in the deformation mapping area should include the use of substantially more data points for the creation of deformation maps, and compression tests to total true strains which are less than that associated with the onset of steady-state for more direct observation of microstructural evolution. Such an approach may lead the development of a more realistic model of hot-working processes.

Summary

1. There is no discernable difference between the flow behavior of as-HIP P/M Rene'95 as a function of particle size. The flow curves of the three materials exhibit a rapid work hardening followed by a gradual flow softening due to dynamic recrystallization. Strain rate sensitivities calculated for peak flow stress indicate stage III deformation over the range of temperatures and strain rates in this study.

2. The three as-HIP materials are microstructurally similar after deformation to a true strain of 0.50. Prior powder particles are still present, having undergone relatively little deformation while areas surrounding them dynamically recrystallized. Strain gradients created between prior powder particles and areas surrounding them are believed to be the cause of non-uniform deformation behavior at low temperatures and high strain rates.

3. Deformation maps based on efficiency values derived from only three strain rates offer inconsistent correlation with observed flow behavior and resultant microstructure. Future work in this area should incorporate larger test matrices with a corresponding increase in microstructural analysis, so as to generate more meaningful hot-working models.

Acknowledgement

The authors gratefully acknowledge the Wyman-Gordon Co. of North Grafton, MA for their support of this study.

References

1. "High Temperature Deformation Behavior of P/M Rene'95," Superalloys 1984, eds. M. Gell et al. (Warrendale, PA: The Metallurgical Society, 1984), 275-284.
2. A.Y. Kandeil et al., "Flow Behavior of Mar M200 Powder Compacts During Isothermal Forging," Metal Science, 14(10)(1980) 493-499.
3. R.G. Menzies, J.W. Edington, G.J. Davies, "Superplastic Behavior of Powder Consolidated Nickel-Base Superalloy IN-100," Metal Science, 15(5)(1981) 210-216.
4. J.-P.A. Immarigeon, P.H. Floyd, "Microstructural Instabilities During Superplastic Forging of a Nickel-Base Superalloy Compact," Met. Trans. A,12A(7)(1981) 1177-1186.
5. Y.V.R.K. Prasad et al., "A New Systems Approach to Dynamic Modeling of Material Behavior in Metal-Working Processes" (Paper published in proceedings of the Titanium Net Shape Technologies Conference, Los Angeles, CA, 26 February - 1 March 1984), 279-289.
6. C.T. Sims, N.S. Stoloff, W.C. Hagel, ed., Superalloys II (New York, NY: John Wiley & Sons, 1987), 453.
7. H.L. Gegel, "Synthesis of Atomistic and Continuum Modeling to Describe Microstructure" (USAF Wright Aeronautical Labs, Wright-Patterson AFB).
8. J.C. Malas, "A Thermodynamic and Continuum Approach to the Design and Control of Precision Forging Processes" (M.S. thesis, Wright State University, 1985).